Gracilin A derivatives target early events in Alzheimer's disease: *in vitro* effects on neuroinflammation and oxidative stress

Rebeca Alvariño[1], Eva Alonso[1,2*], Mikail E. Abbasov[3], Christian M. Chaheine[3], Michael L. Conner[3], Daniel Romo[3], Amparo Alfonso[1], Luis M. Botana[1]

[1] Departamento de Farmacología, Facultad de Veterinaria, Universidad de Santiago de Compostela, Lugo 27003, Spain

[2] Fundacion Instituto de Investigacion Sanitario Santiago de Compostela (FIDIS), Hospital Universitario Lucus Augusti, Lugo 27003, Spain

[3] Department of Chemistry and Biochemistry, Baylor University, One Bear Place #97348, Waco, TX 76798, United States

Abstract

The search for compounds capable of targeting early pathological changes of Alzheimer`s disease (AD), such as oxidative stress and neuroinflammation, is an important challenge. Gracilin A derivatives were recently synthesized, using a pharmacophore-directed retrosynthesis strategy, and found to posses potent neuroprotective effects. In this work, the derivatives 21a, 27a, 27b, 29a, 21b, 22 and 23c (**1-7**) that had demonstrated mitochondrial-mediated, anti-oxidant effects, were chosen. The ability of compounds to modulate the expression of anti-oxidant genes (*CAT*, *GPx*, *SOD's* and *Nrf2*) was determined in SH-SY5Y cells, being the simplified derivatives **2** and **3** the most effective compounds. The anti-neuroinflammatory properties of derivatives were assessed in BV2 microglial cells activated with lipopolysaccharide (LPS). Derivatives decreased the release of cytokines (Il-1β, IL-6, GM-CSF and TNF-α) and other damaging molecules (ROS, NO). Compounds also regulated the translocation of Nrf2 and NFκB, and reduced p38 activation. These protective effects were confirmed in a trans-well co-culture with both cell lines, in which derivatives added to BV2 cells increased SH-SY5Y survival. This work provides new results that demonstrate the neuroprotective properties of gracilin A derivatives, making them promising

candidate drugs for AD. Particularly, derivatives **2** and **3** showed the greatest potential as lead compounds for further development.

Keywords: gracilin, neuroinflammation, anti-oxidant, Alzheimer's disease, Nrf2, neuroprotection

1. Introduction

Marine sponges are a rich source of natural products with biological properties such as anti-inflammatory[1] or neuroprotective[2] effects. These sessile organisms from the phylum Porifera produce several secondary metabolites with defensive functions against pathogens, predators or for space competition. Many of these bioactive molecules have been used as drug leads [3, 4] and some synthetic derivatives have been approved for clinical use or have progressed until Phase II/III clinical trials[5].

Gracilin A is a rare norditerpene that belongs to a family of natural compounds isolated from the marine sponge *Spongionella gracilis*[6]. Gracilin A has been reported to inhibit the activity of phospholipase A2[7] and to possess immunosuppressive and neuroprotective properties. In particular, the compound mimicked the immunosuppressive activity of cyclosporine A by targeting cyclophilin A (CypA)[8]. This natural product was also found to protect neurons from oxidative damage by activating the nuclear factor E2-related factor 2 (Nrf2)[9], blocking the opening of the mitochondrial permeability transition pore (mPTP) [10] and reducing tau hyperphosphorylation[11]. These latter effects are probably related to the affinity for CypD of this family of compounds[12]. In view of these interesting bioactivities, a recently described structure-activity relationship study, that employed a pharmacophore-directed retrosynthesis strategy towards gracilin A, led to identification of key structural requirements for both immunosuppressive and neuroprotective effects, yielding derivatives with selective neuroprotective properties devoid of immunosuppressive effects and *vice versa* [13].

Oxidative stress is an early event in neurodegenerative pathologies like Alzheimer's disease (AD), produced by an increase in reactive oxygen species (ROS) and a reduction in the effectiveness of the endogenous anti-oxidant defenses. ROS accumulation causes damage to DNA, lipids and proteins that can lead to the death of neurons [14]. This cellular event is related to several pathological processes of the illness such as mitochondrial dysfunction, amyloid-beta deposition (Aβ), tau hyperphosphorylation, mPTP opening or neuroinflammation[15, 16]. In this sense, the upregulation of anti-oxidant systems has been proposed as a good strategy to prevent neurodegeneration. The transcription factor Nrf2 triggers one of the most important anti-oxidant pathways, being responsible of the regulation of several genes that encode detoxifying enzymes including superoxide dismutases (SOD's), catalase (CAT), glutathione peroxidases (GPx's) or glutathione transferase[17].

The activation of microglia, the immune cells of the central nervous system, also occurs in early stages of AD[18]. ROS, Aβ and hyperphosphorylated tau accumulation produces a toxic environment that induces the stimulation of these cells. At first, activated microglia remove Aβ by phagocytosis, but the prolonged exposure to toxic molecules produces their chronic activation and the sustained release of toxic cytokines such as interleukin-1β (IL-1β), interleukin-6 (IL-6) or tumor necrosis factor- α (TNF-α) that can produce the death of neighbouring neurons[19]. Microglial are very ductile cells with a great range of phenotypic states [20-22] whose extremes are represented by the toxic phenotype M1 and the protective phenotype M2. M1/M2 model is a simplified way to explain the broad phenotypic spectrum of microglia, although it does not capture all the complexity of these cells. M1 cells release toxic factors such as pro-inflammatory cytokines, ROS and nitric oxide (NO) and are characterized by the activation of the transcription factor kappa-light-chain-enhancer of activated B cells (NFκB), the key controller of the inflammatory response. On the other hand, the opposite phenotype M2 presents neuroprotective characteristics, including release of anti-inflammatory cytokines and the activation of Nrf2[23]. The immunomodulation of microglia, rather than completely blocking their activity, has emerged as a therapeutic strategy to treat AD[24].

In view of our previous results with gracilin A derivatives, the most promising compounds were selected to test their ability to target the anti-oxidant systems of neuronal cells. Moreover, their potential to modulate the phenotypic state of microglia was evaluated with the murine BV2 cell line.

2. Results

3.1 Gracilin A derivatives upregulate anti-oxidant genes in SH-SY5Y cells

Our previous work demonstrated that gracilin A derivatives **2**, **3, 4** and **7** protected SH-SY5Y cells from H_2O_2-induced damage by increasing cell survival, improving mitochondrial membrane potential, decreasing ROS levels and recovering GSH content[13]. Furthermore, compounds **2**, **3**, **4**, and **6** were found to block the opening of the mPTP by inhibiting CypD activity, with compounds **2**, **3**, **4** displaying selectivity for this protein over CypA. The ability of compounds **1** and **5** to decrease oxidative stress and mitochondrial dysfunction has been also demonstrated. Both derivatives protected neuroblastoma cells from H_2O_2-induced damage (Figure S1) and derivative **5** inhibited mPTP opening by targeting CypD (Figure S2). In view of these results, we decided to study the effect of the these derivatives in the expression of anti-oxidant genes. Seven compounds were chosen for this study: the simplified gracilin A derivatives **1**-**3** and the more complex derivatives **4**-**7** (Figure 1).

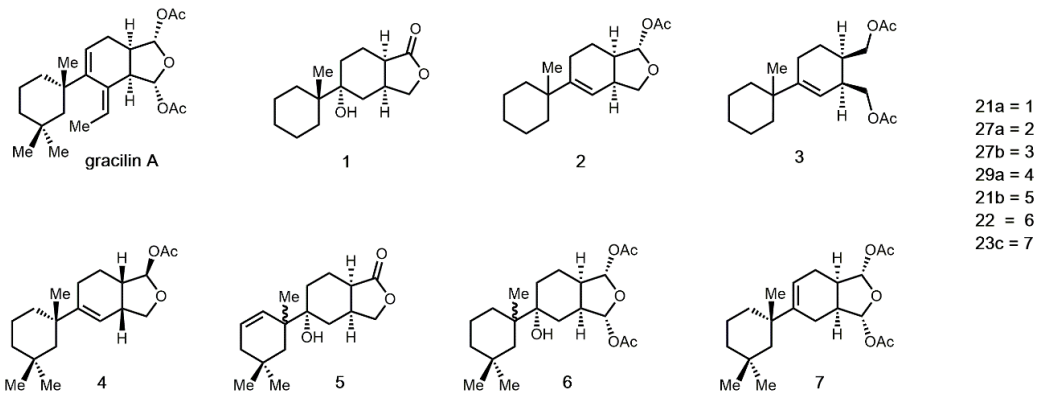

Figure 1. Chemical structures of gracilin A and derivatives

SH-SY5Y human neuroblastoma cells were treated with these derivatives at the most effective concentrations in our previous assays (**1**, **3**, **4**, **6** and **7** were used at 0.01 and 0.1 μM, whereas **2** and **5** were added at 0.1 and 1 μM). Then, 150 μM H_2O_2 was added for 6 h and the relative expression of five genes (*CAT*, *GPx1*, *Nrf2*, *SOD1* and *SOD2*) was determined. Results were calculated with ΔΔCt method using H_2O_2 control cells as calibrator, so the x-axes represent the expression levels of neuroblastoma cells treated with H_2O_2 alone (Figure 2). With regard to *CAT*, compounds **1**, **2** and **3** produced a significant increase in the enzyme gene expression, whereas derivatives **6** and **7** significantly downregulated *CAT* expression (Figure 2a). This reduction is probably due to the addition of H_2O_2, since CAT converts this molecule into water and oxygen and is probably being consumed in this reaction. *GPx1* expression was also increased when SH-SY5Y cells were treated with gracilin derivatives (Figure 2b). Derivatives **3**, **4**, **6** and **7** significantly augmented the enzyme gene expression at 0.01 μM (p<0.001), **2** at 0.1 μM (p<0.001) and **5** at 1 μM (p<0.001). *SOD1*, the cytosolic enzyme isoform, was significantly upregulated by **2** at 0.1 μM (p<0.001), **3** at 0.01 μM (p<0.001) and 0.1 μM (p<0.01) and **7** at 0.01 μM (p<0.01) compared to cells treated only with H_2O_2 (Figure 2c). On the other hand, the expression of the mitochondrial isoform (*SOD2*) was increased by derivatives **1**, **3** and **6** at 0.01 μM (p<0.001) and by compounds **4**, **7** and **5** at the highest concentration (p<0.001). Surprisingly, compound **2** produced a decrease in *SOD2* expression (Figure 2d). Finally, the expression levels of the transcription factor *Nrf2*, responsible of the regulation of anti-oxidant genes, were also determined (Figure 2e). Compounds **2** (0.1 μM), **3** (0.01 μM), **5** (0.1 μM), **6** (0.01 and 0.1 μM) and **7** (0.1 μM) were able to increase *Nrf2* expression. These results suggest that the anti-oxidant properties of gracilin A derivatives are mediated by the upregulation of the genetic expression of phase-II detoxifying enzymes, with compounds **2** and **3** as the most effective. Derivative **3** was particularly interesting because it was able to increase the expression levels of all genes analysed.

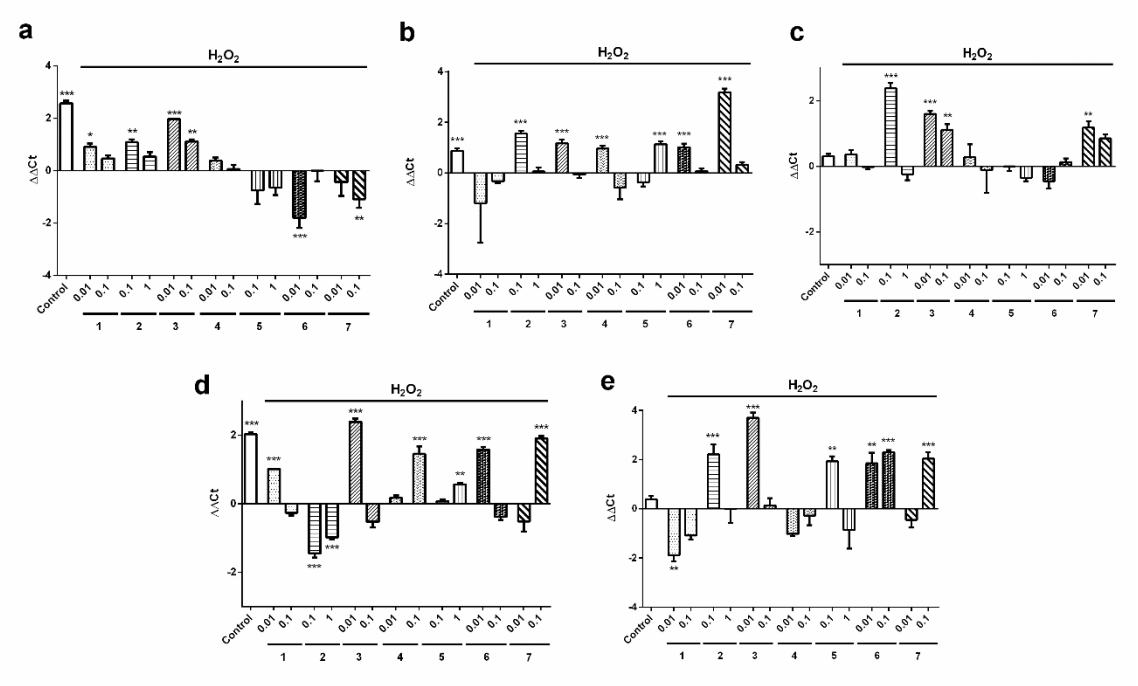

Figure 2. Relative expression of anti-oxidant genes in neuroblastoma cells treated with gracilin A derivatives. 150 µM H_2O_2 and compounds at µM concentrations were added to SH-SY5Y cells for 6 h and their effect on the expression of (a) *catalase*, (b) *glutathione peroxidase 1*, (c) *superoxide dismutase 1*, (d) *superoxide dismutase 2* and (e) *Nrf2* was evaluated. *RPL0* was used as internal normalization control. Relative gene expression was calculated with ΔΔCt method. Cells treated only with H_2O_2 were used as calibrator and are represented by x-axes. Data are expressed as mean ±SEM of three independent replicates performed by duplicate and compared to H_2O_2 control cells by one way ANOVA and Dunnett's tests. *p<0.05. **p<0.01, *** p<0.001

3.2 Compounds reduce the release of pro-inflammatory factors by BV2 microglial cells

BV2 murine microglial cells have been established as a good model for testing the anti-inflammatory properties of compounds[25]. Moreover, LPS from the outer membrane of Gram-negative bacteria has been widely used to activate the inflammatory response in microglia[26, 27]. For neuroinflammation assays, the most effective concentrations of the compounds in our previous assays were chosen. Compounds **1** and **3** were added at 0.01 and 0.1 µM, whereas **5** was used at 0.1 and 1 µM. Otherwise, derivatives **2** (0.1 µM), **4**, **6** and **7** (0.01 µM) were used at a single dose. At first, the effect of gracilin A derivatives on BV2 cells viability was determined

with MTT test. None of the treatments produced a reduction in cell survival after 24 h of incubation (data not shown).

Next, the effect of derivatives on the release of pro-inflammatory cytokines was assessed. Microglial cells were pre-treated with compounds for 1 h and activated with 500 ng/mL LPS for 24 h. Then, the levels of IL-1β, IL-6, TNF-α and granulocyte macrophage colony-stimulating factor (GM-CSF) were monitored in the supernantant (Figure 3). The stimulation with LPS induced a significant increase in IL-1β release (58.2±2.0%, $p<0.001$) with respect to control cells (Figure 3a). All the derivatives produced a significant decrease in this cytokine, reaching levels of resting microglia (between 44.8 and 68.9% of LPS control cells). Due to the positive results obtained with **3** in this assay, the half maximal effective concentration (EC_{50}) was determined. The derivative presented an EC_{50} value of 0.006 μM (CI: 0.001-0.02). With regard to IL-6 release, it was augmented a 55.8±0.7% ($p<0.001$) when BV2 cells were treated with LPS (Figure 3b). The addition of the simplified derivatives **1** (0.01 μM) and **3** (0.01 and 0.1 μM) diminished the cytokine levels until percentages around 82-87%. In general, derivatives reduced TNF-α levels induced by LPS addition (82.7±0.7%, $p<0.001$), with **1**, **5** and **2** as the most effective compounds (Figure 3c). Finally, GM-CSF levels were measured (Figure 3d). Treatment with 500 ng/mL LPS produced an increase of 59.3±1.7 % ($p<0.001$) compared to untreated control cells. The release of GM-CSF was significantly reduced by pre-incubation with **1** at 0.1 (56.3±1.2%, $p<0.05$) and 0.01 μM (61.3±6.1 %, $p<0.01$), **3** at 0.1 μM (52.8 ±4.0%, $p<0.01$) and **5** at 0.1 μM (50.9 ±1.5 %, $p<0.01$). However, compounds **2**, **3** (0.01 μM) and **4** did not decrease GM-CSF levels at statistically significant amounts.

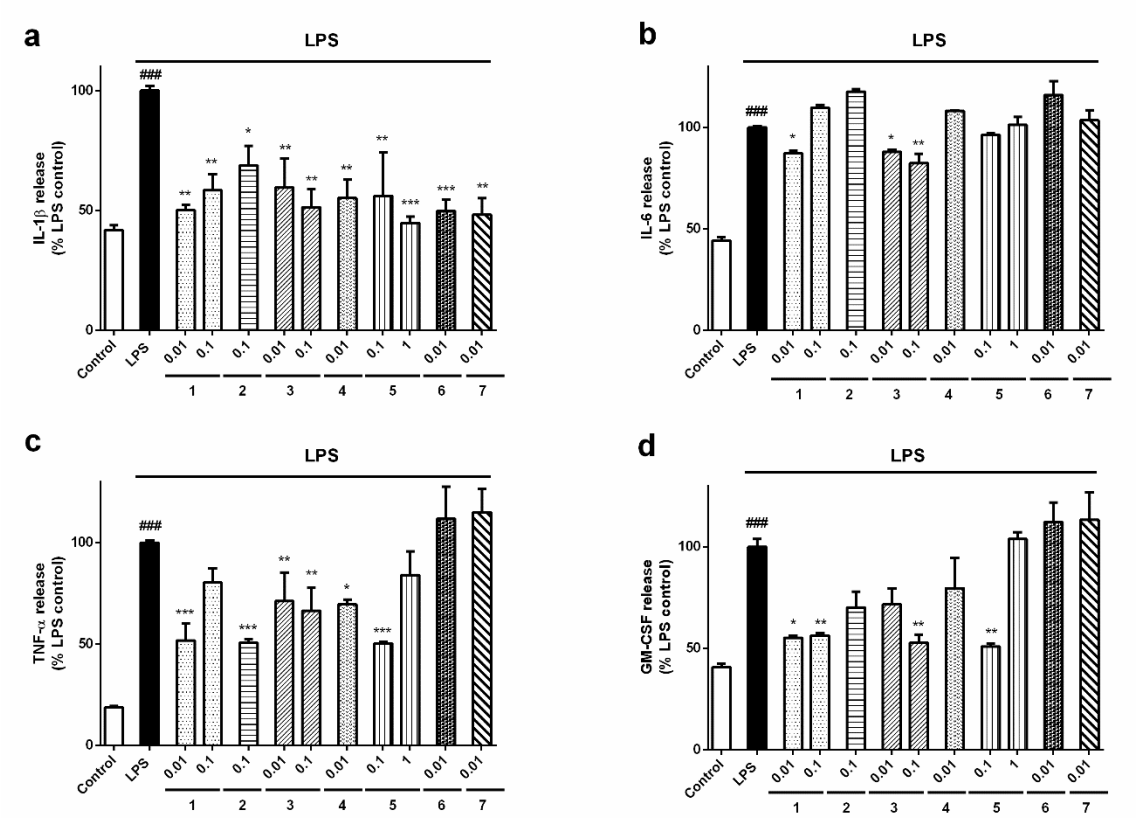

159

160 **Figure 3.** Effect of *Spongionella* synthetic derivatives on cytokine release by microglia. BV2
161 cells were pre-treated with compounds at μM concentrations for 1 h and activated with 500 ng/mL
162 LPS for 24 h. (a) IL-1β, (b) IL-6, (c) TNF-α and (d) GM-CSF levels in the medium of microglial
163 cells were analysed with a Mouse Inflammatory 4-Plex Panel. Data are presented as percentage
164 of LPS control cells. Results are mean± SEM of three independent experiments and compared to
165 cells treated with LPS alone by one way ANOVA and Dunnett's tests. *p<0.05, **p<0.01,
166 ***p<0.001. LPS control cells are compared to inactivated control cells. ###p<0.001

167

168 Neurotoxic microglia are also characterized by augmented levels of ROS and NO. The
169 combination of these molecules can generate the highly toxic species peroxynitrite ($ONOO^-$),
170 which easily crosses cellular membranes and induces neuronal death[28]. The effects of gracilin A
171 derivatives over ROS and NO release were also determined (Figure 4). When microglial cells
172 were stimulated with 500 ng/mL LPS, a significant ROS levels augmentation was observed (136.9

±2.2 %, p<0.01) compared to inactivated cells (Figure 4a). Interestingly, all gracilin A derivatives reduced ROS release. The highest decrease was generated by compounds **2** (35.3 ±1.6 %, p<0.001) and **1** (37.8±4.0 % and 40.0 ±8.0 %, p<0.001). Regarding NO, stimulation with LPS augmented the levels of the toxic factor up to 164.5 ±4.4 % (p<0.001) with respect to control microglial cells (Figure 4b). Pre-treatment with compounds **1** at 0.01 (74.2 ±7.5%, p<0.01) and 0.1 µM (76.4±4.8 %, p<0.05), **2** at 0.1 µM (74.6±6.7%, p<0.01), **3** at 0.01 (62.2±1.7%, p<0.001) and 0.1 µM (76.0 ±4.2 %, p<0.05), **4** at 0.01 µM (76.8±6.4 %, p<0.05) and **5** at 1 µM (62.5±0.3%, p<0.001) significantly reduced NO release by BV2 cells to the medium.

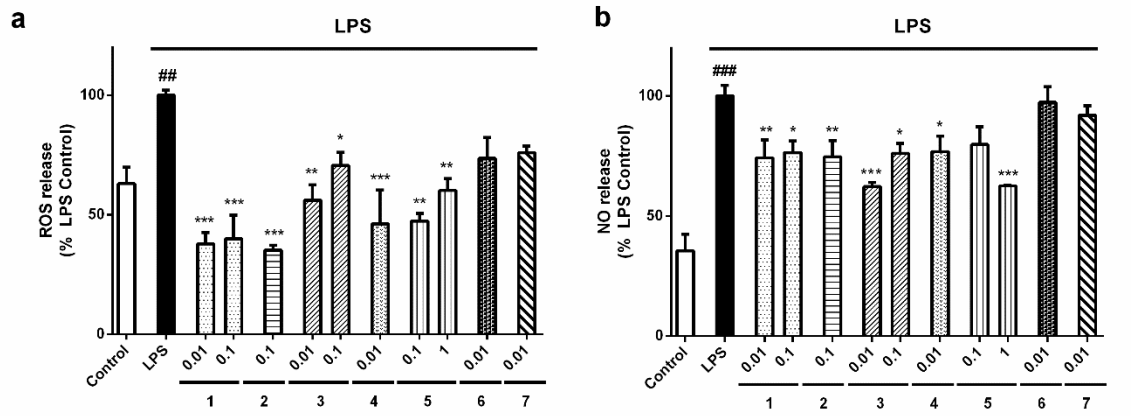

Figure 4. Compounds decreased ROS and NO produced by microglia. BV2 cells were stimulated with 500 ng/mL LPS after pre-treatment with derivatives at µM concentrations for 1 h. After this time, the levels of (a) ROS and (b) NO were measured. Values are mean± SEM of three replicates performed by triplicate and expressed as percentage of LPS control cells. Statistical significance was determined with one way ANOVA test followed by Dunnett's post-hoc test. LPS control cells are compared to inactivated microglia (##p<0.01, ###p<0.001). Treatments with compounds are compared to cells treated only with LPS (*p<0.05, **p<0.01, ***p<0.001).

192 *3.3 Gracilin A derivatives decrease iNOS expression and p38 MAPK activation in microglia*

193 In view of the decrease in NO levels produced by compounds, we decided to measure the
194 expression of iNOS, the enzyme responsible of NO production. BV2 cells were treated as
195 described above, lysed, and the expression levels of the protein were determined by western blot
196 (Figure 5a). Resting microglia expressed the enzyme at only 10.2±1.2% (p<0.001) of the levels
197 expressed by LPS-treated cells. All the derivatives reduced iNOS expression, but the decrease
198 produced by **2**, **5** and **6** was not statistically significant, with levels between 64.4-73.1%. On the
199 other hand, derivatives **4** and **7** at 0.01 μM (26.2±10.6 %, p<0.001; 53.2 ±11.6%, p<0.01,
200 respectively), **1** at 0.01 and 0.1 μM (39.5±6.4 % and 47.4±5.9%, p<0.01, respectively) and **3** at
201 the same concentrations (52.6±13.0%, p<0.01; 36.7±7.0%, p<0.001, respectively), significantly
202 diminished iNOS levels.

203 Activation of MAPK kinases has been related to the neurotoxicity of microglia. Particularly, p38
204 is upregulated in AD brains [29] and its blockage supresses the release of pro-inflammatory
205 cytokines[30]. In this context, the ability of gracilin A derivatives to diminish the activation of p38
206 MAPK kinase was evaluated (Figure 5b). Interestingly, compounds **6**, **7**, **2** and **3** were able to
207 reduce the activity of the enzyme. LPS addition produced an increase in p38 activation of
208 34.1±6.5% (p<0.05) that compounds **6** and **7** diminished up to 59% (p<0.01). Compound **2**
209 decreased the phosphorylated state of the kinase until 55.9±4.0% (p<0.01). Finally, **3** diminished
210 p38 phosphorylation at 0.01 (47.5±4.2%, p<0.001) and 0.1 μM (70.3±5.8%, p<0.05).

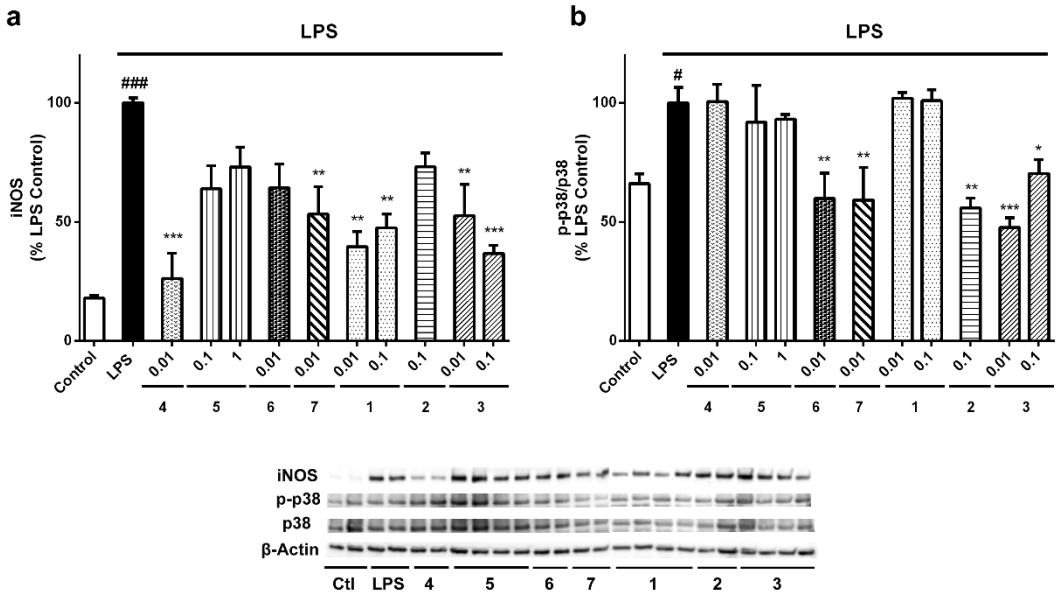

211

212 **Figure 5.** Effects of gracilin A derivatives on iNOS and p38 MAPK. Microglial cells were treated
213 with compounds at μM concentrations and 500 ng/mL LPS. Then, BV2 cells were lysed and the
214 protein expression levels of (a) iNOS and (b) p38 were analysed by western blot. The activation
215 of the kinase was determined as the ratio between phosphorylated and total protein levels. Protein
216 expression levels were corrected by β-actin. Treatments are reordered to match with blots. Values
217 are mean± SEM of three independent experiments carried out by duplicate. Treatments with
218 derivatives are compared to LPS control cells by one way ANOVA and Dunnett's test (*p<0.05,
219 **p<0.01, ***p<0.001). Cells treated with LPS alone are compared to untreated control cells
220 (#p<0.05, ###p<0.001)

221 *3.4 NFκB-p65 and Nrf2 translocation in microglia is modulated by derivatives*

222 The transcription factors NFκB and Nrf2 are related to the phenotypic state of microglia [23]. We
223 tested if the synthetic derivatives of gracilin A were affecting the translocation of both proteins
224 to the nucleus of microglia. With this purpose, the expression levels of Nrf2 and NFκB-p65 in
225 nuclear and cytosolic fractions were studied by western blot (Figure 6). Nrf2 expression in the
226 nucleus decreased when LPS was added to the cells (55.7±10.3%, p<0.05). Pre-incubation with
227 all the derivatives produced a significant increase in the nuclear levels of the transcription factor
228 (Figure 6a). Compound **1** at 0.1 μM augmented the protein expression until 128.4±20.0 %

(p<0.01) of control cells. Derivatives **2** (0.1 μM) and **3** (0.01 μM) also induced an increase in Nrf2 nuclear expression (134.0±6.9% and 147.0±14.4%, p<0.01, respectively). The highest effect on Nrf2 activation was produced by compound **4**, reaching a percentage of 219.4±28.2% (p<0.001). The more complex derivatives **5** (0.1 μM), **6** (0.01 μM) and **7** (0.01 μM) also augmented Nrf2 translocation to the nucleus, with levels of 138.5±9.6% (p<0.05), 174.2±19.9% (p<0.001) and 129.4±8.2% (p<0.01), respectively. The cytosolic expression of the protein was significantly increased in BV2 cells treated with LPS (207.8±17.8%, p<0.001) compared to inactivated microglia, but none of the treatments with derivatives presented significant differences with LPS control cells (Figure 6b).

NFκB-p65 nuclear increase is related to the activation of this pathway and the consequent induction of the pro-inflammatory cascade[23]. LPS addition produced an augmentation in p65 nuclear levels of 45.0±3.2% (p<0.01) (Figure 6c). Pre-treatment with **1** at 0.1 μM diminished the protein expression until a 66.9±4.7% (p<0.05) of LPS control cells. The addition of derivatives **2** (45.0±10.5%, p<0.01), **3** at both concentrations (49.0±3.1%, p<0.01 and 61.5±6.9%, p<0.05, respectively), **4** (57.7±3.4%, p<0.05), **6** (55.4±4.2%, p<0.01) and **7** (59.8±8.5%, p<0.05) also decreased the expression of the pro-inflammatory protein in the nucleus of microglia. Otherwise, p65 cytosolic levels did not present any statistical differences between treatments (Figure 6d).

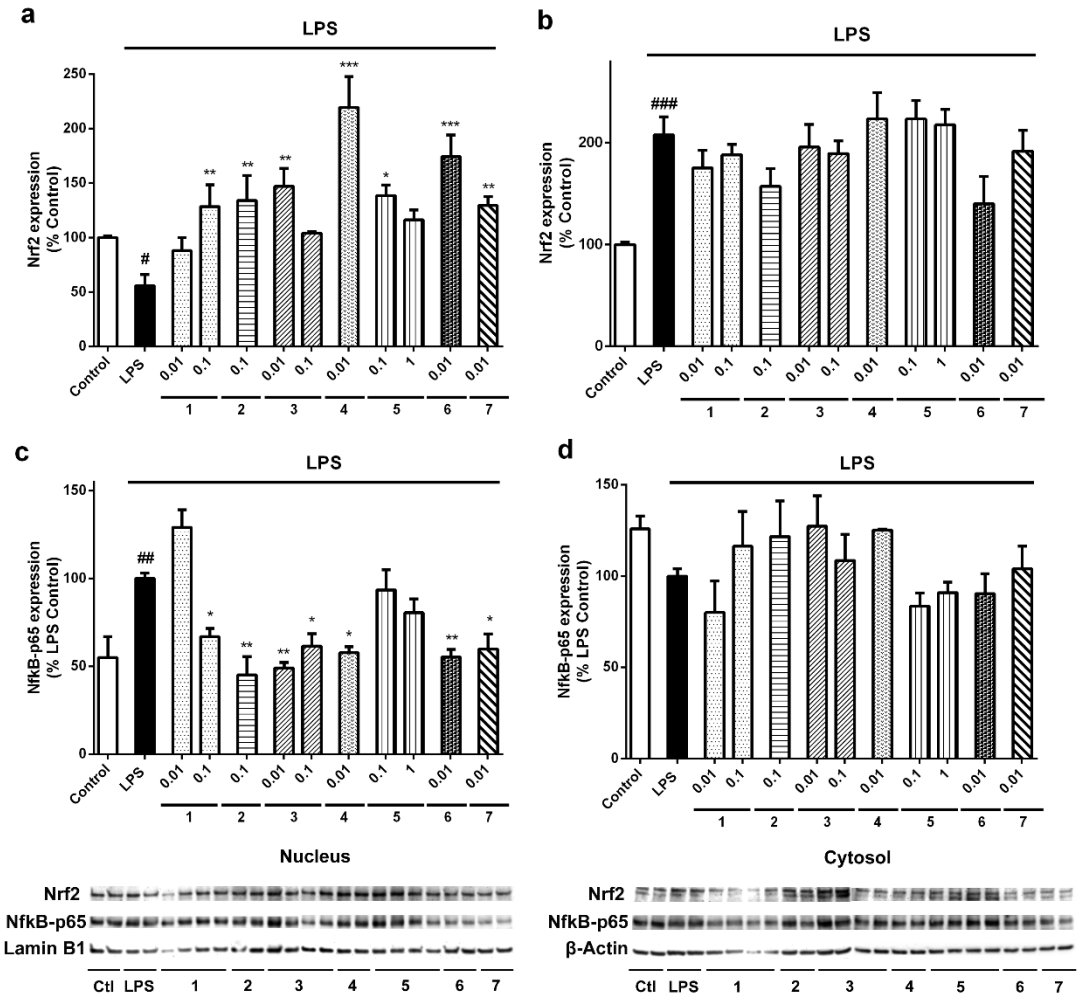

Figure 6. Gracilin A derivatives modulated the expression of Nrf2 and NFκB-p65 in microglia. BV2 murine cells were pre-treated with compounds at μM concentrations for 1 h. Then, LPS was added for 24 h in order to activate the cells. The expression levels of Nrf2 were measured in (a) the nucleus and (b) the cytosol. In the same way, NFκB-p65 expression was determined in (c) nuclear and (d) cytosolic fractions. Protein levels were normalized with lamin B1 and β-actin in the nucleus and the cytosol, respectively. Results are mean± SEM of three replicates performed by duplicate. Statistical differences were calculated with one way ANOVA and Dunnett's test. Treatments with compounds are compared to LPS control cells (*p<0.05, **p<0.01, ***p<0.001) and LPS control cells are compared to inactivated cells (#p<0.05, ##p<0.01, ###p<0.001)

3.5 Compounds protect neuroblastoma cells from microglial-induced injury

Finally, the anti-neuroinflammatory properties of gracilin A derivatives were tested in a trans-well co-culture system with SH-SY5Y and BV2 cells. Neuronal cells were seeded in 24-well plates and microglia was placed in culture inserts above the wells. At first, the effect of the treatments on neuroblastoma survival, without the presence of BV2 cells, was assessed. None of the treatments affected SH-SY5Y viability (data not shown). Therefore, in the trans-well co-culture, microglia was pre-treated with derivatives and stimulated with LPS for 24 h. Then, SH-SY5Y viability was evaluated with MTT assay (Figure 7). The activation of microglia with LPS produced a significant decrease in neuroblastoma survival (82.0±4.5%, $p<0.01$) with respect to SH-SY5Y cells co-cultured with inactivated microglia. The addition of derivatives significantly protected neuroblastoma cells from the damage induced by activated microglial cells: compounds **1** at 0.01 and 0.1 μM (113.1±8.7% and 102.4±4.5%, $p<0.05$, respectively), **2** at 0.1 μM (103.5±3.9%, $p<0.05$), **3** at 0.1 and 0.01 μM (99.2±0.9% and 104.9±7.4 %, $p<0.05$, respectively), **4** at 0.01 μM (107.7±7.6%, $p<0.05$), **5** at 0.1 μM (112.9±12.5%, $p<0.05$), **6** at 0.01 μM (113.1±9.3 %, $p<0.05$) and **7** at 0.01 μM (105.3±4.0 %, $p<0.05$) improved SH-SY5Y survival, agreeing with our previous results.

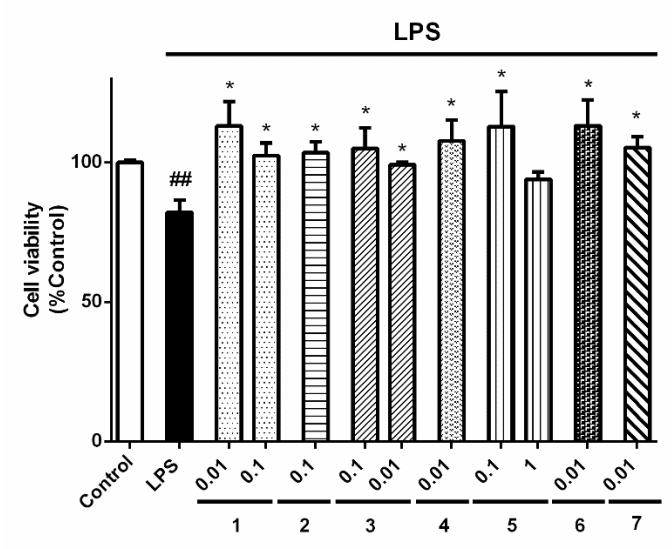

Figure 7. Gracilin A derivatives protected SH-SY5Y cells from activated microglia in a trans-well co-culture. BV2 cells were seeded in inserts placed above SH-SY5Y cells. Microglia was

277 pre-treated with compounds at μM concentrations for 1 h and activated with 500 ng/mL LPS
278 during 24 h. Then, the viability of neuroblastoma cells was determined with MTT assay. Values
279 are mean± SEM of three independent experiments carried out by duplicate. Results are expressed
280 as percentage of SH-SY5Y cells co-cultured with inactivated microglia (control). One way
281 ANOVA and Dunnett's tests were used to analyse the statistical differences between treatments
282 and neuroblastoma cells co-cultured with BV2 cells treated with LPS alone (LPS) (*p<0.05). LPS
283 cells are compared to control cells (##p<0.01).

284 ## 3. Discussion

285 AD is the most common neurodegenerative disease, characterized by loss of synapses and
286 neurons, which produces cognitive decline, memory impairment and even death. The incidence
287 rate of AD doubles every 5 years after the age of 65 and it is estimated to reach more than 115
288 million cases in 2050[31]. Current AD-approved drugs improve patient's symptoms but do not
289 modify the progression of the illness[32]. The failure of new drugs for AD in clinical trials has been
290 attributed to the complex nature of the pathology and to the fact that the disease should be treated
291 in earlier stages[33, 34]. Emerging data suggest that the beginning of the disorder occurs many years
292 before the appearance of the symptoms[35]. Specifically, oxidative stress and neuroinflammation
293 have been reported in AD transgenic mouse brains before the accumulation of Aβ and misfolded
294 tau protein[36, 37]. The results presented in this work suggest that gracilin A derivatives are able to
295 attenuate oxidative stress and neuroinflammation, early events in AD onset.

296 Our previous work demonstrated the anti-oxidant and neuroprotective properties of gracilin A
297 derivatives [13]. In this study, we confirmed that the neuroprotective activity of *Spongionella*
298 derivatives is related to their ability to increase anti-oxidant enzymes expression. *CAT*, *SOD's*
299 and *GPx1* gene expression was upregulated when gracilin A derivatives were present. Moreover,
300 the transcription factor *Nrf2*, a key target in neurodegeneration, was augmented by these
301 compounds. As described previously, Nrf2 translocation to the nucleus induces the expression of
302 many genes related to the endogenous anti-oxidant system. Otherwise, Nrf2 expression increase

303 could be related to the improvement of mitochondrial function produced by gracilin A derivatives
304 [13], as the transcription factor also upregulates genes related to pyruvate metabolism, glycolysis
305 and gluconeogenesis [38], and enhances mitochondrial respiration, with the consequent recovery of
306 mitochondrial membrane potential[39].

307 In AD brains, microglia are dysregulated and release toxic factors like ROS, pro-inflammatory
308 cytokines, chemokines and NO that contribute to the deleterious environment observed in the
309 illness and promote neuronal death[19]. NO is produced by iNOS, a enzyme highly expressed in
310 microglia from AD patients. NO reacts with superoxide anion and generates peroxynitrite, a
311 highly cytotoxic molecule that leads to lipid peroxidation, S-nitrosylation of proteins and
312 mitochondrial damage[28]. The regulation of iNOS occurs at transcriptional level and there are
313 many transcription factors involved, being NFκB the most important one[40]. Its activation produces
314 the release of pro-inflammatory cytokines (IL-1β, IL-6, TNF-α, or interferon-γ). IL-1β is essential
315 in the initiation of the immune response and is known to increase the production of other
316 neurotoxic mediators including ROS, NO and cytokines[41]. In addition, increased TNF-α levels
317 have been detected in AD brains and anti-inflammatory drugs altering both TNF-α levels and
318 NFκB signalling have displayed promising results in clinical trials[42]. Thus, the reduction of pro-
319 inflammatory markers related to M1 phenotype (ROS, NO and cytokines) and the inhibition of
320 NFκB pathway is a good therapeutic approach for AD treatment. Otherwise, NFκB and Nrf2
321 transcription factors are closely interconnected, as they are redox sensitive. Increased ROS levels
322 lead to the activation of NFκB and the pro-inflammatory M1 phenotype of microglial cells. On
323 the other hand, redox homeostasis is tightly controlled by Nrf2, which provides anti-oxidant
324 protection to microglia and triggers the neuroprotective M2 phenotype. Therefore, the modulation
325 of these transcription factors, specifically NFκB downregulation and Nrf2 upregulation, results
326 in the attenuation of the toxic microglial phenotype in favor of the neuroprotective phenotype[23].

327 The abnormal activation of MAPK kinases has been detected in brains and peripheral cells of AD
328 patients[29, 43]. Particularly, p38 MAPK plays an important role in the illness. The kinase promotes
329 chronic neuroinflammation because it contributes to the regulation of iNOS, TNF-α and IL-1β in

microglia and astrocytes. p38 also enhances tau hyperphosphorylation through its ability to directly phosphorylate specific sites of the protein, or indirectly by increasing IL-1β secreted by microglia, which in turn augments the activation of neuronal p38[44]. Thus, the inhibition of this central pathway in AD by gracilin A derivatives **2**, **3**, **6** and **7** contributes to their anti-neuroinflammatory activity. *Spongionella* –derived synthetic compounds diminished the levels of toxic molecules released by microglia (ROS, NO, pro-inflammatory cytokines), being especially effective compounds **1**, **2**, **3**, and **4**. These derivatives modulated microglial cells towards the M2 protective phenotype by inhibiting NFκB and activating Nrf2. Interestingly, compounds **6** and **7** only decreased IL-1β release, the cytokine that initiates the inflammatory cascade. These derivatives also blocked p38 and NFκB and activated Nrf2, but did not affect the other pro-inflammatory markers analysed, suggesting that **6** and **7** were also modulating the phenotypic state of microglia, but their effects occurred more slowly. Finally, the protection shown by compounds when neuroblastoma cells were co-cultured with microglia confirmed their ability to modulate neuroinflammation.

Overall, the monoacetoxy furanose **2** and the diacetate **3** presented the best results in our assays. These derivatives were able to upregulate the anti-oxidant defences of neuronal cells (*CAT*, *SOD's*, *GPx1* and *Nrf2*) and to protect them in the presence of activated microglia by modulating the phenotypic state of the immune cells. These results, together with the mitochondria-related protective effects previously reported [13], open an interesting field for further studies against AD with these promising compounds. New studies will help to understand the connection between the anti-neuroinflammatory and mitochondrial-related effects of gracilin A-derivatives.

4. Material and methods

4.1 Chemicals and solutions

5-(and-6)-carboxy-2′, 7′-dichlorodihydrofluorescein diacetate (carboxy-H_2DCFDA), Dulbecco´s Modified Eagle´s medium: Nutrient Mix F-12 (DMEM/F-12), Roswell Park Memorial Institute 1640 medium (RPMI 1640), fetal bovine serum (FBS), trypsin/EDTA, penicillin- streptomycin, Griess Reagent Kit, Mouse Inflammatory 4-Plex Panel, Supersignal West Pico Luminiscent

Substrate and Supersignal West Femto Maximum Sensitivity Substrate were purchased from Thermo Fisher Scientific (Waltham, MA, USA). Primers were obtained from Integrated DNA Technologies (Iowa, USA). Aurum™ Total RNA Mini Kit and Taq™ Universal SYBR Green Supermix were purchased from Bio-Rad Laboratories (Barcelona, Spain). Other chemicals used were reagent grade and purchased from Sigma-Aldrich (Madrid, Spain).

4.2 Compound information

Gracilin A derivatives were initially synthesized in the Department of Chemistry and Biochemistry at Baylor University employing gracilin A as a natural product lead. Structural elucidation of compounds was based on complete spectroscopic characterization and for this study gracilin A derivatives were resynthesized using synthetic methods previously described [13].

4.3 Cell culture

Human neuroblastoma SH-SY5Y cell line was obtained from American Type Culture Collection (ATCC), number CRL2266. Cells were cultured in DMEM/F-12 supplemented with 10% FBS, 1% glutamax, 100 U/mL penicillin and 100 µg/mL streptomycin.

BV2 murine microglial cell line was purchased from Interlab Cell Line Collection (ICLC), number ATL03001. Cells were maintained in RPMI 1640 medium with 10 % FBS, 100 U/mL penicillin and 100 µg/mL streptomycin.

Cell lines were maintained at 37 C in a humidified atmosphere of 5% CO_2 and 95% air and dissociated using 0.05% trypsin/EDTA.

4.4 Quantitative PCR

Table 1. Primer sequences used in qPCR

Gene	Accesion Number	Primer sequence
Catalase (*CAT*)	NM_001752	5′-GAAGTGCGGAGATTCAACACT -3′ 5′-ACACGGATGAACGCTAAGCT -3′
Glutathione peroxidase 1 (*GPx1*)	BC007865	5′-CCGACCCCAAGCTCATCA -3′ 5′-TTCTCAAAGTTCCAGGCAACATC-3′
Nuclear factor E2-related factor 2 (*Nrf2*)	NM_001313903	5′-ACACGGTCCACAGCTCATC-3′ 5′-TGTCAATCAAATCCATGTCCTG-3′
Superoxide dismutase 1 (*SOD1*)	NM_000454	5′- TCATCAATTTCGAGCAGAAGG-3′ 5′-TGCTTTTTCATGGACCACC-3′
Superoxide dismutase 2 (*SOD2*)	NM_000636	5′-CATCAAACGTGACTTTGGTTC -3′ 5′-CTCAGCATAACGATCGTGGTT-3′
Ribosomal protein lateral stalk subunit P0 (*RPLP0*)	NM_001002	5′-GGAGCCAGCGAAGCCACACT-3′ 5′-CACATTGCGGACACCCTCTA-3′

SH-SY5Y cells were treated with compounds and 150 μM H_2O_2 for 6 h. Then, total RNA was obtained with the Aurum™ Total RNA Mini Kit following the manufacturer's instructions. RNA concentration and purity were determined using a Nanodrop™ 2000 spectrophotometer (Thermo Fisher Scientific). cDNA was synthetized with 0.5 μg of RNA, oligo-dT primers and RevertAid Reverse Transcriptase (Thermo Fischer Scientific), following manufacturer's instructions. Quantitative PCR was performed using iTaq™ Universal SYBR Green Supermix in a Step-One real-time PCR system (Applied Biosystems). cDNA was amplified with specific primers (Table 1) for *catalase* (*CAT*), *superoxide dismutase 1* (*SOD1*), *superoxide dismutase 2* (*SOD2*), *glutathione peroxidase 1* (*GPx1*) and *nuclear factor (erythroid-derived 2)-like 2* (*Nrf2*). Data were analysed with the Step-One software (Applied Biosystems). *Ribosomal protein lateral stalk subunit P0* (*RPLP0*) was used as internal normalization control and relative quantification was performed using ΔΔCt method. Cells treated only with 150 μM H_2O_2 were used as calibrator. Experiments were carried out in triplicate at least three independent times.

4.5 Measurement of reactive oxygen species levels

Experiments with BV2 microglial cells were performed as previously described[45]. The levels of ROS were quantified with the fluorescence dye carboxy-H_2DCFDA (5-(and-6)-carboxy-2′, 7′-dichlorodihydrofluorescein diacetate). BV2 microglial cells were pre-treated with the compounds for 1 h and 500 ng/mL LPS during 24 h. After this time, cells were washed twice with serum-free

400 medium and 20 μM carboxy-H_2DCFDA was added. Cells were incubated for 1 h at 37°C and pre-
401 warmed PBS was added to each well for 30 min. The fluorescence was read at 527 nm, with an
402 excitation wavelength of 495 nm. The assay was carried out in triplicate, three independent times.

403 *4.6 Nitric oxide release assay*

404 BV2 murine microglial cells were seeded in DMEM without phenol red in 12-well plates at a
405 density of 1x 10^6 cells per well. Microglia were treated as described above and the release of NO
406 to the medium was measured with a Griess Reagent Kit, following manufacturer's instructions.
407 Briefly, 150 μL of cell supernatant were mixed with 20 μL of Griess reagent and 130 μL of
408 deionized water. After 30 min of incubation at room temperature, the absorbance was read at 548
409 nm in a spectrophotometer plate reader. The experiments were performed at least three times.

410 *4.7 Measurement of cytokines release*

411 BV2 cells were treated with compounds for 1 h and activated with 500 ng/mL LPS for 24 h. Then,
412 the supernatant was collected to analyse the levels of cytokines. The release of IL-1β, IL-6, TNF-
413 α and GM-CSF to the medium was determined with a Mouse Inflammatory 4-Plex Panel. The
414 assay was carried out following manufacturer's instructions. Luminex 200 ™ instrument and
415 xPONENT® software (LuminexCorp, Austin, TX) were used to collect the data.

416 *4.8 Protein extraction*

417 BV2 cells were treated with compounds for 1 h and stimulated with 500 ng/mL LPS during 24 h.
418 Then, cells were rinsed twice with ice-cold PBS and a hypotonic buffer was added (20 mM Tris-
419 HCl pH 7.4, 10 mM NaCl and 3 mM $MgCl_2$, containing a phosphatase/protease inhibitor
420 cocktail). Cells were incubated for 15 min on ice and centrifuged at 3000 rpm, 4 °C for 15 min.
421 The supernatant was collected as the cytosolic fraction and the pellet was resuspended in a nuclear
422 extraction solution (100 mM Tris pH 7.4, 2 mM Na_3VO_4, 100 mM NaCl, 1% Triton X-100, 1 mM
423 EDTA, 10% glycerol, 1 mM EGTA, 0.1% SDS, 1 mM NaF, 0.5% deoxycholate, and 20 mM
424 $Na_4P_2O_7$, containing 1 mM PMSF and a protease inhibitor cocktail). Lysates were incubated on

ice for 30 min with vortexing intervals of 10 min. Then, samples were centrifuged at 14000 g, 4°C for 30 min and the nuclear fraction was obtained. Cytosolic fraction was quantified with Direct Detect system (Merck Millipore) and nuclear protein concentration was determined with Bradford method.

4.9 Western blot assays

Electrophoresis was carried out in 4-20% sodium dodecyl sulphate polyacrylamide gels (Biorad) with 20 or 10 µg of cytosolic or nuclear protein, respectively. Snap i.d. system (Merck Millipore) was used for membrane blocking and antibody incubation. Anti-Nrf2 (1:1000, Millipore), anti-NFκB-p65 (1:10000, Abcam), anti-iNOS (1:1000, Abcam), anti-phospho-p38 (1:1000, Abcam) and anti-p38 (1:1000, Abcam) were used for the evaluation of protein expression and signal was normalized using anti-lamin B1 (1:2000, Abcam) and anti-β-actin (1:2000, Millipore) for nuclear and cytosolic fractions, respectively. Activation of p38 kinase was calculated as the ratio of phosphorylated and total protein levels. Protein bands were detected with Supersignal West Pico Luminiscent Substrate and Supersignal West Femto Maximum Sensitivity Substrate and Diversity GeneSnap system and software (Syngene, Cambridge, U.K.).

4.10 Trans-well co-culture

SH-SY5Y neuroblastoma cells were cultured in 24-well plates at 5x 10^5 cells per well. BV2 microglial cells were seeded in culture inserts (0.4 µM pore size, Merck-Millipore) placed above neuroblastoma cells at a density of 2.5 x10^5 cells per insert. Both cell lines were allowed to grow for 24 h. Then, BV2 cells were pre-treated with gracilin A derivatives for 1 h and 500 ng/mL LPS were added to each insert for 24 h. The effect over SH-SY5Y survival was determined with MTT (3-(4, 5-dimethyl thiazol-2-yl)-2, 5-diphenyl tetrazolium bromide) assay. Cells were washed three times with saline buffer and incubated with 500 µg/mL MTT for 1 h at 37°C and 300 rpm. Then, 5% sodium dodecyl sulphate was added to each well to dissolve the formazan crystals. Absorbance was measured at 595 nm in a spectrophotometer plate reader. The experiment was performed at least three times.

4.11 Statistical analysis

Data are presented as mean ± SEM. Differences were evaluated by one way ANOVA with Dunnett's post hoc test and statistical significance was considered at $p < 0.05$.

Supplementary information

Neuroprotective effects of gracilin A derivatives **1** and **5** in an oxidative stress model with SH-SY5Y cells. Effects of cell viability, mitonchondrial membrane potential, ROS and GSH levels, mitochondrial permeability transition pore opening and inhibition of cyclophilin D activity.

AUTHOR INFORMATION

Corresponding Author

*Email: eva.alonso@usc.es. Phone/Fax: +34982822233

Author Contributions

R. A. performed *in vitro* experiments. M.E.A, C.M.C., M.C. and D.R. synthesized and characterized gracilin A derivatives. E. A., A. A. and L.M.B. did critical discussion and experimental design. The manuscript was written with the contribution of all authors.

Notes

The authors declare no competing financial interest

Acknowledgments

The research leading to these results has received funding from the following FEDER cofunded-grants. From Consellería de Cultura, Educación e Ordenación Universitaria Xunta de Galicia, 2017 GRC GI-1682 (ED431C 2017/01). From CDTI and Technological Funds, supported by Ministerio de Economía, Industria y Competitividad, AGL2014-58210-R, AGL2016-78728-R (AEI/FEDER, UE), ISCIII/PI16/01830 and RTC-2016-5507-2, ITC-20161072. From European Union POCTEP 0161-Nanoeaters -1-E-1, Interreg AlertoxNet EAPA-317-2016, Interreg Agritox

EAPA-998-2018 and H2020 778069-EMERTOX. Support from NIH (R37 GM052964 to D.R.) and the Robert A. Welch Foundation (AA-1280 to D.R.) is also gratefully acknowledged.

References

1. Ciaglia, E.; Malfitano, A. M.; Laezza, C.; Fontana, A.; Nuzzo, G.; Cutignano, A.; Abate, M.; Pelin, M.; Sosa, S.; Bifulco, M.; Gazzerro, P., Immuno-Modulatory and Anti-Inflammatory Effects of Dihydrogracilin A, a Terpene Derived from the Marine Sponge Dendrilla membranosa. *Int J Mol Sci* **2017,** *18* (8).
2. Alghazwi, M.; Kan, Y. Q.; Zhang, W.; Gai, W. P.; Yan, X. X., Neuroprotective Activities of Marine Natural Products from Marine Sponges. *Curr Med Chem* **2016,** *23* (4), 360-82.
3. Brackovic, A.; Harvey, J. E., Synthetic, semisynthetic and natural analogues of peloruside A. *Chem Commun (Camb)* **2015,** *51* (23), 4750-65.
4. Grandic, M.; Frangez, R., Pathophysiological effects of synthetic derivatives of polymeric alkylpyridinium salts from the marine sponge, Reniera sarai. *Mar Drugs* **2014,** *12* (5), 2408-21.
5. Andersen, R. J., Sponging off nature for new drug leads. *Biochem Pharmacol* **2017,** *139*, 3-14.
6. Rateb, M. E.; Houssen, W. E.; Schumacher, M.; Harrison, W. T.; Diederich, M.; Ebel, R.; Jaspars, M., Bioactive diterpene derivatives from the marine sponge Spongionella sp. *J Nat Prod* **2009,** *72* (8), 1471-6.
7. Nirmal, N.; Praba, G. O.; Velmurugan, D., Modeling studies on phospholipase A2-inhibitor complexes. *Indian J Biochem Biophys* **2008,** *45* (4), 256-62.
8. Sanchez, J. A.; Alfonso, A.; Rodriguez, I.; Alonso, E.; Cifuentes, J. M.; Bermudez, R.; Rateb, M. E.; Jaspars, M.; Houssen, W. E.; Ebel, R.; Tabudravu, J.; Botana, L. M., Spongionella Secondary Metabolites, Promising Modulators of Immune Response through CD147 Receptor Modulation. *Front Immunol* **2016,** *7*, 452.
9. Leirós, M.; Sánchez, J. A.; Alonso, E.; Rateb, M. E.; Houssen, W. E.; Ebel, R.; Jaspars, M.; Alfonso, A.; Botana, L. M., Spongionella secondary metabolites protect mitochondrial function in cortical neurons against oxidative stress. *Mar Drugs* **2014,** *12* (2), 700-18.
10. Sanchez, J. A.; Alfonso, A.; Leiros, M.; Alonso, E.; Rateb, M. E.; Jaspars, M.; Houssen, W. E.; Ebel, R.; Botana, L. M., Spongionella Secondary Metabolites Regulate Store Operated Calcium Entry Modulating Mitochondrial Functioning in SH-SY5Y Neuroblastoma Cells. *Cell Physiol Biochem* **2015,** *37* (2), 779-92.
11. Leirós, M.; Alonso, E.; Rateb, M. E.; Houssen, W. E.; Ebel, R.; Jaspars, M.; Alfonso, A.; Botana, L. M., Gracilins: Spongionella-derived promising compounds for Alzheimer disease. *Neuropharmacology* **2015,** *93*, 285-93.
12. Du, H.; Guo, L.; Zhang, W.; Rydzewska, M.; Yan, S., Cyclophilin D deficiency improves mitochondrial function and learning/memory in aging Alzheimer disease mouse model. *Neurobiol Aging* **2011,** *32* (3), 398-406.
13. Abbasov, M. E.; Alvarino, R.; Chaheine, C. M.; Alonso, E.; Sanchez, J. A.; Conner, M. L.; Alfonso, A.; Jaspars, M.; Botana, L. M.; Romo, D., Simplified immunosuppressive and neuroprotective agents based on gracilin A. *Nat Chem* **2019,** *11* (4), 342-350.
14. Wojsiat, J.; Zoltowska, K. M.; Laskowska-Kaszub, K.; Wojda, U., Oxidant/Antioxidant Imbalance in Alzheimer's Disease: Therapeutic and Diagnostic Prospects. *Oxid Med Cell Longev* **2018,** *2018*, 6435861.
15. Kalani, K.; Yan, S. F.; Yan, S. S., Mitochondrial permeability transition pore: a potential drug target for neurodegeneration. *Drug Discov Today* **2018**.

16. Prasad, K. N., Simultaneous activation of Nrf2 and elevation of antioxidant compounds for reducing oxidative stress and chronic inflammation in human Alzheimer's disease. *Mech Ageing Dev* **2016,** *153*, 41-7.
17. Dinkova-Kostova, A. T.; Kostov, R. V.; Kazantsev, A. G., The role of Nrf2 signaling in counteracting neurodegenerative diseases. *Febs j* **2018**.
18. Bagyinszky, E.; Giau, V. V.; Shim, K.; Suk, K.; An, S. S. A.; Kim, S., Role of inflammatory molecules in the Alzheimer's disease progression and diagnosis. *J Neurol Sci* **2017,** *376*, 242-254.
19. von Bernhardi, R.; Eugenin-von Bernhardi, L.; Eugenin, J., Microglial cell dysregulation in brain aging and neurodegeneration. *Front Aging Neurosci* **2015,** *7*, 124.
20. Friedman, B. A.; Srinivasan, K.; Ayalon, G.; Meilandt, W. J.; Lin, H.; Huntley, M. A.; Cao, Y.; Lee, S. H.; Haddick, P. C. G.; Ngu, H.; Modrusan, Z.; Larson, J. L.; Kaminker, J. S.; van der Brug, M. P.; Hansen, D. V., Diverse Brain Myeloid Expression Profiles Reveal Distinct Microglial Activation States and Aspects of Alzheimer's Disease Not Evident in Mouse Models. *Cell Rep* **2018,** *22* (3), 832-847.
21. Rangaraju, S.; Dammer, E. B.; Raza, S. A.; Rathakrishnan, P.; Xiao, H.; Gao, T.; Duong, D. M.; Pennington, M. W.; Lah, J. J.; Seyfried, N. T.; Levey, A. I., Identification and therapeutic modulation of a pro-inflammatory subset of disease-associated-microglia in Alzheimer's disease. *Mol Neurodegener* **2018,** *13* (1), 24.
22. Keren-Shaul, H.; Spinrad, A.; Weiner, A.; Matcovitch-Natan, O.; Dvir-Szternfeld, R.; Ulland, T. K.; David, E.; Baruch, K.; Lara-Astaiso, D.; Toth, B.; Itzkovitz, S.; Colonna, M.; Schwartz, M.; Amit, I., A Unique Microglia Type Associated with Restricting Development of Alzheimer's Disease. *Cell* **2017,** *169* (7), 1276-1290.e17.
23. Rojo, A. I.; McBean, G.; Cindric, M.; Egea, J.; Lopez, M. G.; Rada, P.; Zarkovic, N.; Cuadrado, A., Redox control of microglial function: molecular mechanisms and functional significance. *Antioxid Redox Signal* **2014,** *21* (12), 1766-801.
24. Pena-Altamira, E.; Prati, F.; Massenzio, F.; Virgili, M.; Contestabile, A.; Bolognesi, M. L.; Monti, B., Changing paradigm to target microglia in neurodegenerative diseases: from anti-inflammatory strategy to active immunomodulation. *Expert Opin Ther Targets* **2016,** *20* (5), 627-40.
25. Gresa-Arribas, N.; Vieitez, C.; Dentesano, G.; Serratosa, J.; Saura, J.; Sola, C., Modelling neuroinflammation in vitro: a tool to test the potential neuroprotective effect of anti-inflammatory agents. *PLoS One* **2012,** *7* (9), e45227.
26. Han, Q.; Yuan, Q.; Meng, X.; Huo, J.; Bao, Y.; Xie, G., 6-Shogaol attenuates LPS-induced inflammation in BV2 microglia cells by activating PPAR-gamma. *Oncotarget* **2017,** *8* (26), 42001-42006.
27. Ye, J.; Yan, H.; Xia, Z., Oxycodone ameliorates the inflammatory response induced by lipopolysaccharide in primary microglia. *J Pain Res* **2018,** *11*, 1199-1207.
28. Asiimwe, N.; Yeo, S. G.; Kim, M. S.; Jung, J.; Jeong, N. Y., Nitric Oxide: Exploring the Contextual Link with Alzheimer's Disease. *Oxid Med Cell Longev* **2016,** *2016*, 7205747.
29. Sun, A.; Liu, M.; Nguyen, X. V.; Bing, G., P38 MAP kinase is activated at early stages in Alzheimer's disease brain. *Exp Neurol* **2003,** *183* (2), 394-405.
30. Munoz, L.; Ralay Ranaivo, H.; Roy, S. M.; Hu, W.; Craft, J. M.; McNamara, L. K.; Chico, L. W.; Van Eldik, L. J.; Watterson, D. M., A novel p38 alpha MAPK inhibitor suppresses brain proinflammatory cytokine up-regulation and attenuates synaptic dysfunction and behavioral deficits in an Alzheimer's disease mouse model. *J Neuroinflammation* **2007,** *4*, 21.
31. Dubois, B.; Feldman, H. H.; Jacova, C.; Hampel, H.; Molinuevo, J. L.; Blennow, K.; DeKosky, S. T.; Gauthier, S.; Selkoe, D.; Bateman, R.; Cappa, S.; Crutch, S.; Engelborghs, S.; Frisoni, G. B.; Fox, N. C.; Galasko, D.; Habert, M. O.; Jicha, G. A.; Nordberg, A.; Pasquier, F.; Rabinovici, G.; Robert, P.; Rowe, C.; Salloway, S.; Sarazin, M.; Epelbaum, S.; de Souza, L. C.; Vellas, B.; Visser, P. J.; Schneider, L.; Stern, Y.; Scheltens, P.; Cummings, J. L., Advancing research diagnostic criteria for Alzheimer's disease: the IWG-2 criteria. *Lancet Neurol* **2014,** *13* (6), 614-29.

572 32. Sun, B. L.; Li, W. W.; Zhu, C.; Jin, W. S.; Zeng, F.; Liu, Y. H.; Bu, X. L.; Zhu, J.; Yao, X.
573 Q.; Wang, Y. J., Clinical Research on Alzheimer's Disease: Progress and Perspectives. *Neurosci*
574 *Bull* **2018**.
575 33. Rosini, M.; Simoni, E.; Caporaso, R.; Minarini, A., Multitarget strategies in Alzheimer's
576 disease: benefits and challenges on the road to therapeutics. *Future Med Chem* **2016,** *8* (6), 697-
577 711.
578 34. Selkoe, D. J., Preventing Alzheimer's disease. *Science* **2012,** *337* (6101), 1488-92.
579 35. Wirz, K. T.; Keitel, S.; Swaab, D. F.; Verhaagen, J.; Bossers, K., Early molecular changes
580 in Alzheimer disease: can we catch the disease in its presymptomatic phase? *J Alzheimers Dis*
581 **2014,** *38* (4), 719-40.
582 36. Ferretti, M. T.; Bruno, M. A.; Ducatenzeiler, A.; Klein, W. L.; Cuello, A. C., Intracellular
583 Abeta-oligomers and early inflammation in a model of Alzheimer's disease. *Neurobiol Aging*
584 **2012,** *33* (7), 1329-42.
585 37. Mota, S. I.; Costa, R. O.; Ferreira, I. L.; Santana, I.; Caldeira, G. L.; Padovano, C.;
586 Fonseca, A. C.; Baldeiras, I.; Cunha, C.; Letra, L.; Oliveira, C. R.; Pereira, C. M.; Rego, A. C.,
587 Oxidative stress involving changes in Nrf2 and ER stress in early stages of Alzheimer's disease.
588 *Biochim Biophys Acta* **2015,** *1852* (7), 1428-41.
589 38. Esteras, N.; Dinkova-Kostova, A. T.; Abramov, A. Y., Nrf2 activation in the treatment of
590 neurodegenerative diseases: a focus on its role in mitochondrial bioenergetics and function. *Biol*
591 *Chem* **2016,** *397* (5), 383-400.
592 39. Holmstrom, K. M.; Baird, L.; Zhang, Y.; Hargreaves, I.; Chalasani, A.; Land, J. M.;
593 Stanyer, L.; Yamamoto, M.; Dinkova-Kostova, A. T.; Abramov, A. Y., Nrf2 impacts cellular
594 bioenergetics by controlling substrate availability for mitochondrial respiration. *Biol Open* **2013,**
595 *2* (8), 761-70.
596 40. Yuste, J. E.; Tarragon, E.; Campuzano, C. M.; Ros-Bernal, F., Implications of glial nitric
597 oxide in neurodegenerative diseases. *Front Cell Neurosci* **2015,** *9*, 322.
598 41. Fernandez, P. L.; Britton, G. B.; Rao, K. S., Potential immunotargets for Alzheimer's
599 disease treatment strategies. *J Alzheimers Dis* **2013,** *33* (2), 297-312.
600 42. Decourt, B.; Lahiri, D. K.; Sabbagh, M. N., Targeting Tumor Necrosis Factor Alpha for
601 Alzheimer's Disease. *Curr Alzheimer Res* **2017,** *14* (4), 412-425.
602 43. Wang, S.; Zhang, C.; Sheng, X.; Zhang, X.; Wang, B.; Zhang, G., Peripheral expression
603 of MAPK pathways in Alzheimer's and Parkinson's diseases. *J Clin Neurosci* **2014,** *21* (5), 810-4.
604 44. Munoz, L.; Ammit, A. J., Targeting p38 MAPK pathway for the treatment of Alzheimer's
605 disease. *Neuropharmacology* **2010,** *58* (3), 561-8.
606 45. Alvariño, R.; Alonso, E.; Lacret, R.; Oves-Costales, D.; Genilloud, O.; Reyes, F.; Alfonso,
607 A.; Botana, L. M., Streptocyclinones A and B ameliorate Alzheimer's disease pathological
608 processes in vitro. *Neuropharmacology* **2018,** *141*, 283-295.

609

610 **Table of contents**

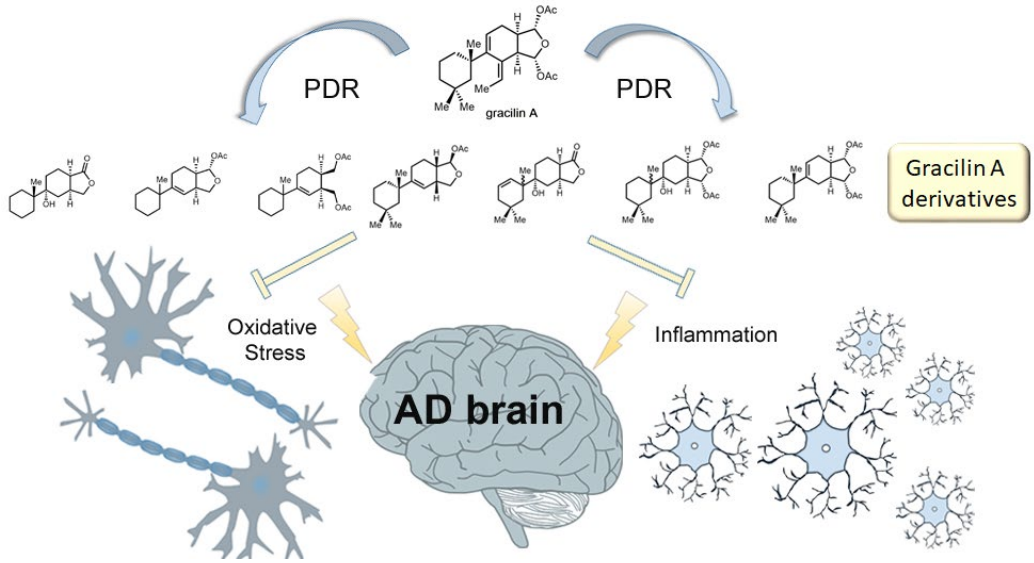

611

612